

Department of Physical Geography and Regional Geographical Analysis  
Faculty of Geography and History  
University of Barcelona

**PhD Thesis**

# **The Western Mediterranean Oscillation and Rainfall in the Catalan Countries**

**Memory presented by**  
**Joan Albert López i Bustins**  
*(Summary)*

**PhD Director**

**Prof. Dr Javier Martín Vide**  
**University de Barcelona**

**Barcelona, June 2007**

# **1<sup>ST</sup> CHAPTER**

## **THE WESTERN MEDITERRANEAN OSCILLATION (WEMO) DEFINITION AND ITS INDEX CALCULATION (WEMOI)**



## 1.1. ANTECEDENTS

The amplitude of the Mediterranean basin favours the presence of a synchronised but opposed behaviour by atmospheric dynamics between its eastern and western sub-basins. This is defined as the Mediterranean oscillation (MO) concept by Conte *et al.* (1989). The MO is a low-frequency variability pattern producing opposing barometric, thermal and pluviometric anomalies between the extremities of the basin. Strongly linked in winter to the northern hemisphere teleconnection modes of the AO and the NAO (Düneloh and Jacobeit, 2003), the MO has been considered the most important regional low-frequency pattern influencing rainfall in the Mediterranean basin by some studies (Düneloh and Jacobeit, 2003; Kutiel *et al.*, 1996; Douguédroit, 1998; Maheras *et al.*, 1999a). The influence of the MO on climate variability has also been analysed in other studies (Corte-Real *et al.*, 1995, Palmieri *et al.*, 2001; Palutikof *et al.*, 1996; Piervitali *et al.*, 1997; Kutiel and Paz, 1998; Maheras *et al.*, 1999b; Brunetti *et al.*, 2002; Xoplaki *et al.*, 2003; Baldi *et al.*, 2004). In a simple way, the MO can be interpreted by two opposite surface pressure (and geopotential height) configurations, in its positive mode by an anticyclone (or an anticyclonic ridge in mid-tropospheric levels) in the western Mediterranean and Iberia, and a low (or a trough) in the eastern Mediterranean. The original Mediterranean index was defined as the difference of standardised geopotential height anomalies at Algiers and Cairo (Conte *et al.*, 1989). Other similar indices are calculated as the difference of standardised pressure anomalies at Gibraltar and the Israelian meteorological station of Lod (Palutikof, 2003) or as the difference between standardised pressure anomalies at Marseille and Jerusalem (Brunetti *et al.*, 2002).

Using canonical correlation analysis to identify the main coupled circulation-rainfall patterns in the Mediterranean basin, Düneloh and Jacobeit (2003) suggest the existence of a Mediterranean meridional circulation (MMC) pattern. It is defined by two opposite pressure centres, one west of Great Britain, near 45-50°N and 20-25°W, and the other on the Italian Peninsula. This pattern produces meridional flows over the Iberian Peninsula, northerly in its positive mode and southerly in its negative one. Baldi *et al.* (2005) define a Mediterranean jet-stream which explains the long dry spells in summer.

There have been other recent contributions to the research of the relationship between the Mediterranean atmospheric dynamics, mainly that in the eastern basin, and that in the rest of Europe. The surface pressure and the 500-hPa geopotential heights over Greece have been particularly correlated with the standard weather types (Lamb's, and Hess and Brezowsky's types) for western and central Europe (Anagnostopoulou *et al.*, 2004; Hatzaki *et al.*, 2004). Some hydrographic works link the MO with the temperature, salinity and density of the

waters in north Adriatic (Grbec *et al.*, 2003; Supić *et al.*, 2004). They introduce an MO index expressly defined by means of the SLP between the best-correlated areas in mid-North Atlantic and south-east Mediterranean with water density in the north Adriatic. In this same direction, Hatzaki *et al.* (2007) have recently defined an Eastern Mediterranean oscillation named EMP (Eastern Mediterranean pattern), which is the detected opposed oscillation between north-eastern North Atlantic and eastern Mediterranean in winter at 300-hPa and 500-hPa levels.

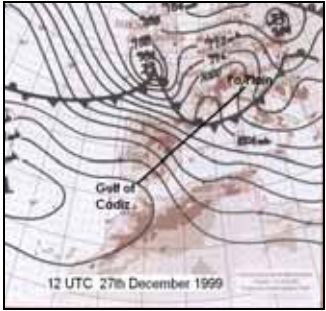
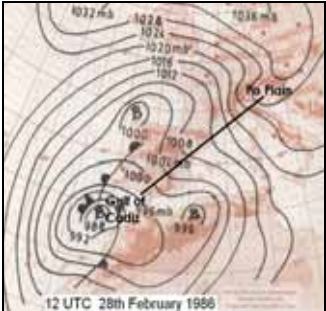


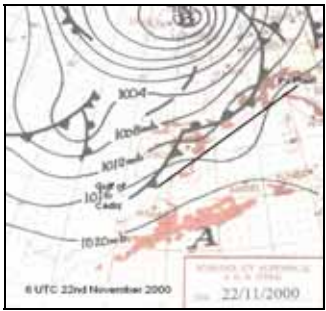
In this thesis, a secondary oscillation form in the western Mediterranean basin is defined, which is able to explain the pluviometric variability in the eastern fringe of the Iberian Peninsula, an area weakly or not related to the NAO pattern (Rodó *et al.*, 1997; Esteban-Parra *et al.*, 1998; Martín-Vide *et al.*, 1999; Martín-Vide and Fernández Belmonte, 2001; Rodríguez-Puebla *et al.*, 2001; Muñoz-Díaz and Rodrigo, 2003, 2004; Trigo *et al.*, 2004; Gallego *et al.*, 2005; Muñoz-Díaz, 2006; Paredes *et al.*, 2006). This might have practical value in downscaling methods. The applications of these methods are essential for the Mediterranean domain to know the climatic variability at high resolution (Goodess and Jones, 2002; Palutikof *et al.*, 2002). The WeMO is mainly presented as an NAO alternative on the Catalan Countries study area. This is a methodology that Kutiel and Benaroch (2002) applied to define a new index due to the weak NAO influence on the eastern Mediterranean basin. The index was named North Sea – Caspian pattern (NCP) and the transect was drawn at 500-hPa, between the North Sea (0°E, 55°N and 10°E, 55°N) and the north Caspian Sea (50°E, 45°N and 60°E, 45°N). The NCP explains better than the NAO the eastern Mediterranean pluviometry (Kutiel *et al.*, 2002), the Turkish one (Kutiel and Türkes, 2005) and those on the Aegean and Black seas (Gunduz and Ozsoy, 2005).

## 1.2. THE WESTERN MEDITERRANEAN OSCILLATION DEFINITION

The different definitions of the MO have always intended to cover mainly the atmospheric dynamics of the entire Mediterranean basin. However, in the new proposal, the WeMO is defined only within the synoptic framework of the western Mediterranean basin and its vicinities. The suggested areas are the Po Plain, in the north of the Italian peninsula, an area with a relatively high barometric variability due to the different influences of the Central European anticyclone and the Liguria Sea low; and the Gulf of Cadiz, in the south-west of the Iberian Peninsula, often subject to the influence of the Azores anticyclone and, episodically, to the cut off of circumpolar lows or to its own cyclogenesis. The transect linking both areas matches more or less the coastline of the Catalan Countries. In this way, the identification of the basic atmospheric circulations will be carried out on the basis of the segment's south-west – north-east orientation. Moreover, in the WeMO definition and its corresponding index (WeMOi) the surface level has been chosen because, for purposes of application to calculate the precipitation on the eastern façade of Iberian Peninsula, the surface flow direction is a determining factor in the case of torrential rainfall (Estrela *et al.*, 2002; Azorín-Molina and López-Bustins, 2004).

The positive phase of the WeMO corresponds to the anticyclone over the Azores enclosing the south-west Iberian quadrant and low-pressures in the Gulf of Genoa; and its negative phase coincides with the Central European anticyclone located north of the Italian peninsula and a low-pressure centre, often cut off from northern latitudes, in the framework of the Iberian south-west. A neutral phase will apply in the case of the low-pressure gradient over the western Mediterranean basin and the surrounding areas, or whenever a north-east or south-west advection with the same isobar is established, linking both areas of the dipole (Figure 1). In case of the north-east flows, the WeMOi might certainly be negative depending on the exact localisation of the action centres, since the most often synoptic situation associated to north-east flows over eastern Iberia is the ubication of the Central European winter anticyclone over northern Italy.

The mean SLP maps for the 1951-2000 period show clearly opposed pressure fields between the Gulf of Cadiz and northern Italy (NOAA-CIRES plots for 15 °W–15 °E, 35 °N–50 °N). Esteban *et al.* (2005), using a daily surface pressure data-grid and multivariable analysis, detected for an area in eastern Iberia, located in the middle of the transect, seven synoptic circulation patterns, four of them clearly showing a WeMO positive phase, and one of them a negative one.

Index phase	Surface pressure in the Gulf of Cadiz	Surface pressure in the Po Plain	Synoptic pattern over the western Mediterranean	Surface synoptic map (real case)
Positive (+)	High	Low	N, NW, WNW and W advections	
Negative (-)	Low	High	ENE, E, ESE and SE advections	
Neutral (~0)	=	=	Low gradient	
			NE advection (exception)	
			SW advection (exception)	

**Figure 1.** Definition of the WeMO phases by means of synoptic real maps (the transect Gulf of Cadiz – Po Plain is drawn). (Maps are from the daily meteorological bulletin of the Spanish Meteorological Office). (Adaptation from Martin-Vide and Lopez-Bustins, 2006).

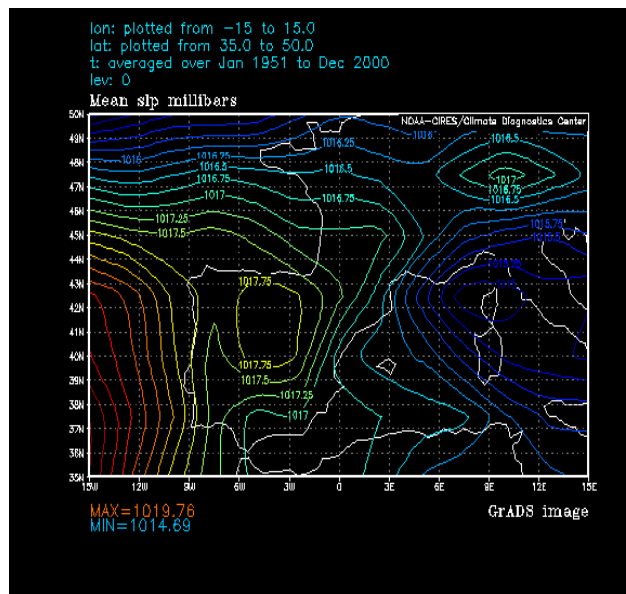


**Figure 2.** Mean SLP plot for the window (15°W-15°E and 35°N-50°N) for the 1951-2000 period (NOAA-CIRES plots).



### 1.3. BAROMETRIC DIPOLE SERIES: PADUA AND SAN FERNANDO (1821-2000)

#### 1.3.1. PADUA

Padua (45°24'N-11°47'E) is the representative one of the Po Valley. This series is one of the longest in Europe. It starts in 1725 with a daily observation. Its history and metadata are described in the edited IMPROVED book (Camuffo and Jones, 2002). The reconstruction of the series within the project was carried out by Dr Camuffo (University of Padua). The series is monthly and annually represented in order to see if some inhomogeneity remains.

##### 1.3.1.1. IMPROVE project data analysis

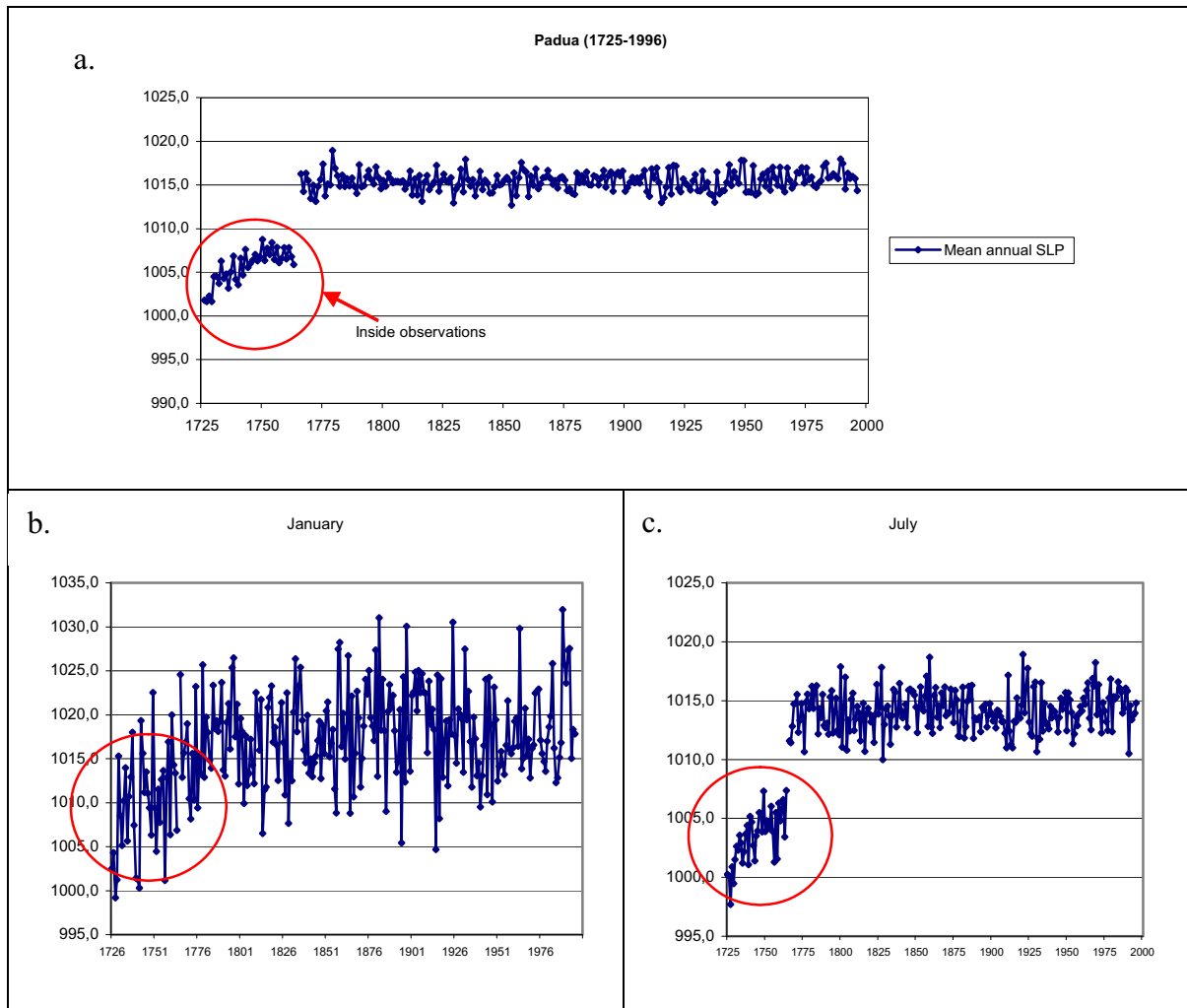
The first data of the Padua series were registered in Sir Poleni house for the 1725-1764 period. Some inhomogeneities were detected in this initial period (Figure 3a). The barometer was inside a room on the first floor (Toaldo 1770; Crestani, 1926). There were some calibration problems using the Amonton's thermometer (Camuffo, 2002). The inhomogeneity was more detectable in summer (Figures 3b and 3c). Camuffo *et al.* (2006) has recently corrected these data after finding out the cause: a displacement of the scale, which included a nearly linear drift and an incorrect position of the reference level.

Toaldo (1770, 1781) presented the data from 1765 to 1769, and since 1768 the measurement was made at the Ezzelino Castle, on the Specola Tower exactly. There is a continuous measurement until 1959. The following years are supplied by different locations in Padua or very near to the city: G. Magrini Observatory of the Water Magistrate, G. Allegri airport, botanic gardens and the CNR (The National Research Council). IMPROVE project just contributed data until November 1997.

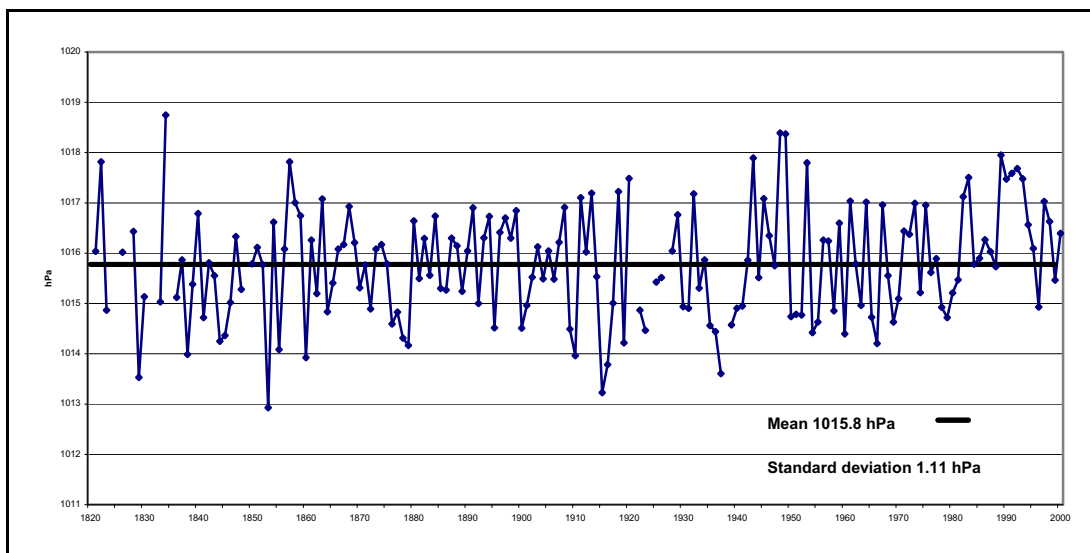
Maugeri *et al.* (2004) using IMPROVE project data detected an inhomogeneity during the last decade of the 20th century. They homogenised all the Padua pressure series at sea-level, but they eliminated some periods, the largest one being the 1990s over the 1821-2000 study period. For the WeMOi calculation I used their daily homogenized Padua series data, but I covered the 1991-2000 period using the Vicenza Air Force database, which is located very near to Padua, to its north-west. The Vicenza pressure series is also reduced to sea-level.

Figure 4 shows the homogenised mean annual SLP in Padua for the 1821-2000 period. In this period, 1.354 days have no WeMOi value (2.06% out of the 65.744 total days), but for

the most interesting period, 1951-2000, only 4 days are lacking. The pressure evolution is without important oscillations. It only increases since 1940, which has been already documented by Maugeri *et al.* (2004) for the entire Po Valley.



**Figure 3.** a. Annual pressure in Padua (IMPROVE project data) (1725-1996) (hPa). b. Idem as (a), but for January. c. Idem as (a), but for July. (Red circles indicate anomalous values).



**Figure 4.** Mean annual SLP in Padua (1821-2000).

### 1.3.2. SAN FERNANDO (CADIZ)

San Fernando (36°17'N-6°07'W) is selected as the representative point of the Gulf of Cadiz. It reflects the atmosphere dynamism between the Azores anticyclone and the polar lows with a south track. This pressure series is officially the longest one of the Iberian Peninsula, and starts at the end of the 18th century; but the treated data are since 1821, because it is when the reliable period begins thanks to the Urrutia Brothers' measurements in Cadiz. From 1870 to the present, the data are from the Navy Observatory in San Fernando, a few kilometres from Cadiz at 29.17 metres above sea-level (a.s.l.) (Figure 5). Within the IMPROVE project, Barriendos *et al.* (2002) collect information about metadata and corrections on this series.



**Figure 5.** Location map of the different points where the long pressure series of Gulf of Cadiz was measured. (From Barriendos *et al.*, 2002).

The San Fernando mean annual SLP is represented (I write San Fernando instead of Cadiz because most of the series comes from the former) to check if there are inhomogenities after the corrections that were applied during the European project research period.

The series looks random until the last decade, where there are several years that are anomalously high (Figure 6). It is necessary to check if these anomalies remain during all year round or just during certain months. Therefore, the mean SLP series is monthly represented (Figure 7).

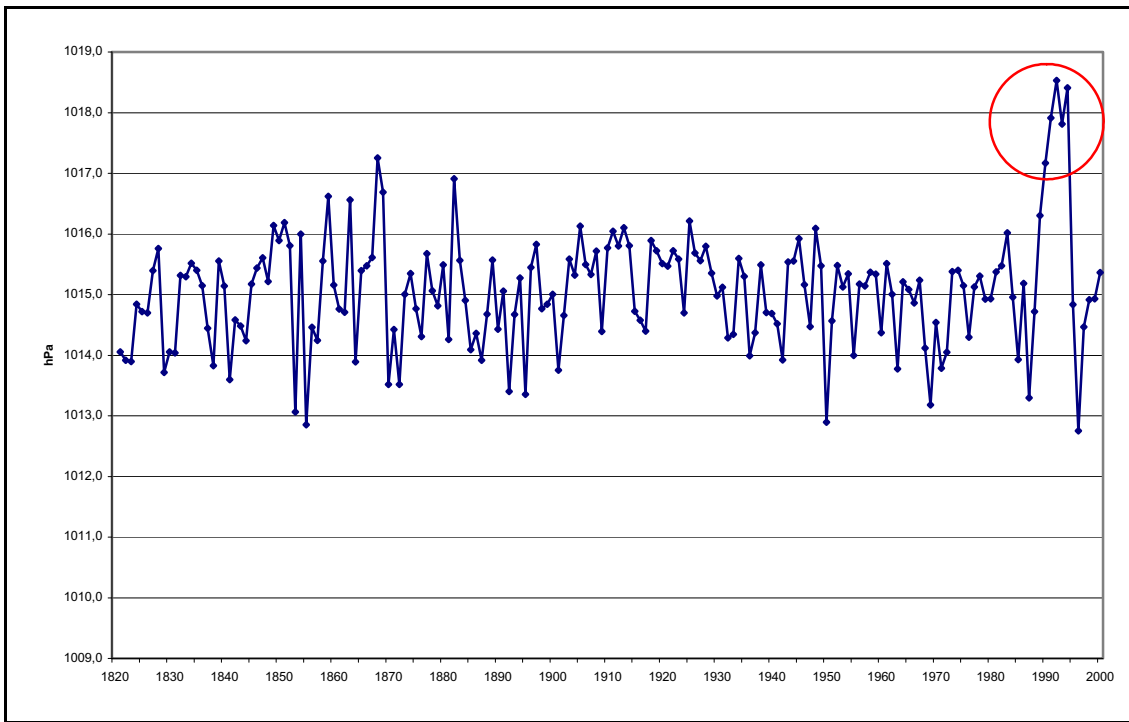


**Figure 6.** Mean annual SLP in San Fernando (1821-2000). (A red circle indicates the anomalous period).

It is during the warm semester (April to September) when the anomalies are detected at the beginning of 1990s. July and August, in the middle of the summer, are the months when the largest anomaly is detected. Another positive anomaly is detected in summer during the Urrutia Brothers's period (1821-1869).

#### 1.3.2.1. Homogenisation of the Urrutia Brothers's period (1821-1869)

The aim is to correct June, July, August and September. The metadata is quite poor, and there is no scrap of evidence about this inhomogeneity. It is probable that Urrutia Brothers lived very few meters a.s.l., and the data from the Navy Observatory are not reduced to sea-level as the *Anales del Instituto* show. The differences are larger in summer when the thermal low over Iberian Peninsula takes place.

The calculations for the homogenisation are carried out using a reference period close to the one to be corrected, 1881-1930 (50 years). There are no remarkable outliers in the four months during this period. To find the additive negative factor we must calculate the mean of the reference period and subtract the mean of the inhomogeneous period, 1821-1869 (49 years). Once the factor is calculated, it must be added to the summer months of this inhomogeneous period (Table 1). Anyway, the Urrutia Brothers's period has not been used in several analyses due to the inhomogeneties detected.

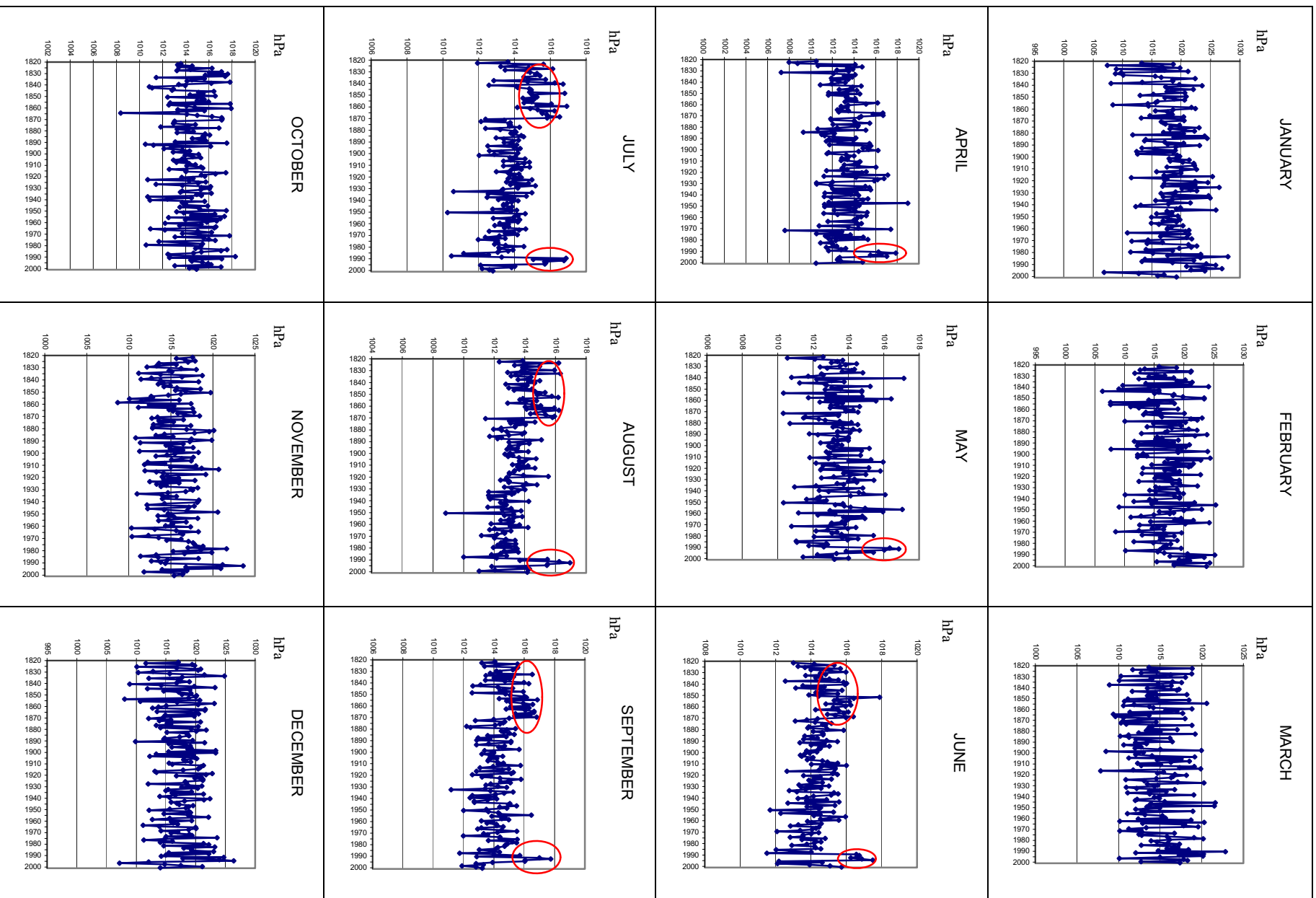


**Figure 7.** Monthly pressure series in San Fernando (1821-2000). (Red ellipses indicate anomalous periods).

	Mean 1881-1930	Mean 1821-1869	Additive factor
<b>June</b>	1014.37	1015.04	-0.6621
<b>July</b>	1013.89	1014.98	-1.0869
<b>August</b>	1013.47	1014.45	-0.9742
<b>September</b>	1014.22	1015.06	-0.8423

**Table 1.** Additive factor calculation to apply to the 1821-1869 inhomogenised period using the 1881-1930 reference period.

### 1.3.2.2. Homogenisation of the beginning of the 1990s period

To homogenize the series, nearby pressure point data are required. Gibraltar (1825-2000) (CRU, Climatic Research Unit) and Lisbon (1855-1995) (CRU and ADVICE project) are available. San Fernando is located between both cities. The mean pressure is calculated between Gibraltar and Lisbon (G+L). Figure 8 shows both G+L and San Fernando series. The latter is confirmed not to be reduced at sea-level. Along the decades there is an equal distance between both series which is broken during the first years of 90s.

There is a very close evolution between both graphical lines during the following years: 1991, 1992, 1993 and 1994. Afterwards, a monthly analysis is carried out to check exactly which months contain the inhomogeneity, comparing the San Fernando and G+L series from January 1988 to December 1995. Corrective factors are calculated for each month of the year. The period 1881-1980 is used to calculate the means of both series. Monthly, the mean G+L pressure is subtracted from the mean San Fernando pressure. Thus, I deduced the monthly pressure mean (hPa) which separate both series. Afterwards, the pressure differences are calculated between both series from January 1988 to December 1995. The corrective factor calculated for each month must be subtracted from this difference.(Table 2). The thresholds -1 and 1 are established to identify the anomalous months. An inhomogeneity is detected when several months consecutively exceed this threshold (Table 3 and Figure 9). Table 2 could have been summarised by means of the following formula for a specific month:  $F_c = ((X_G + X_L)/2) - X_{SF}$ , where  $F_c$  is the corrective factor and  $X$  the pressure mean.

June 1989 to December 1994 is an inhomogeneous period, which is just interrupted during 6 months (from August 1990 to January 1991). To avoid sudden pressure shifts in the daily series due to the use of different corrective factors in consecutive months, the third column in table 3 displays the values to be subtracted in each month individually. This smoothing consists of calculating the corrective values mean of the month to modify, the previous month and the following month.

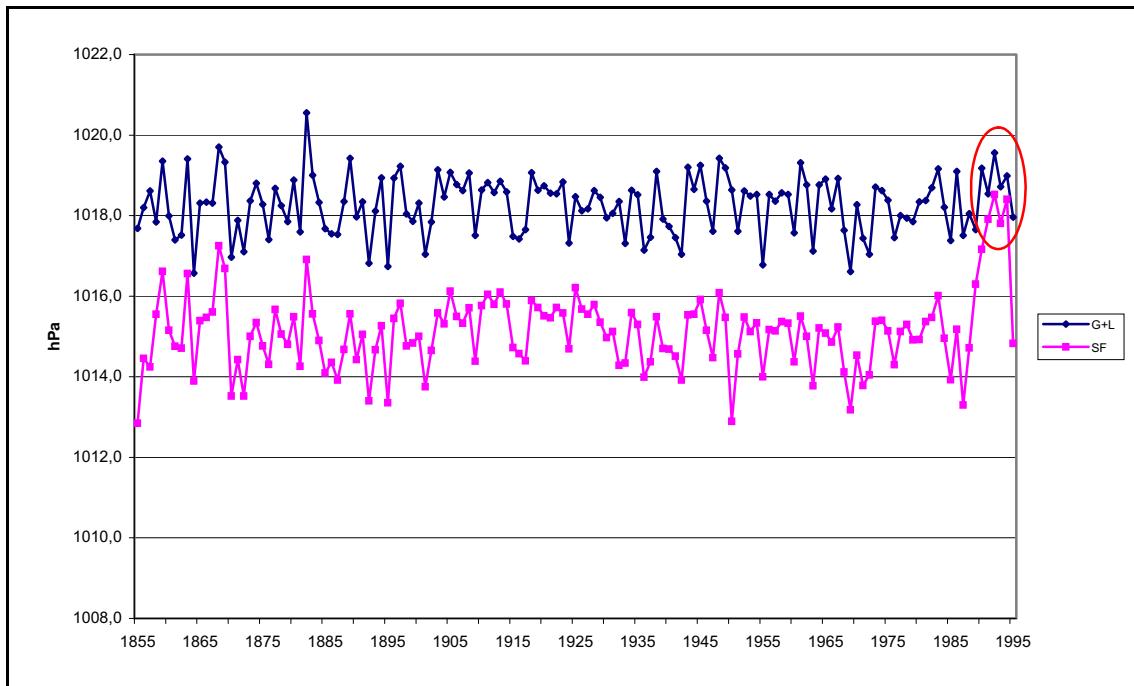


**Figure 8.** San Fernando pressure series (SF) and the mean pressure between Gibraltar and Lisbon (G+L) (1855-1995). (A red ellipse indicates the anomalous values).

1881-1980	San Fernando mean	Gibraltar mean	Lisbon mean	Gibraltar and Lisbon mean	(G+L mean – SF mean) = Corrective Factor (F <sub>c</sub> )
January	1018.5	1022.4	1021.5	1022.0	3.5
February	1017.0	1020.7	1019.7	1020.2	3.2
March	1014.6	1018.2	1016.9	1017.5	2.9
April	1013.4	1016.6	1016.3	1016.5	3.1
May	1013.5	1016.4	1016.5	1016.5	2.9
June	1014.2	1016.7	1017.5	1017.1	2.9
July	1013.7	1016.3	1017.6	1017.0	3.3
August	1013.1	1016.2	1017.2	1016.7	3.7
September	1014.1	1017.6	1017.5	1017.6	3.4
October	1014.5	1018.2	1017.4	1017.8	3.3
November	1015.6	1019.5	1018.6	1019.0	3.4
December	1017.8	1021.6	1020.8	1021.2	3.4

**Table 2.** Mean pressure difference between San Fernando and G+L series during the 1881-1980 period.

The inhomogeneity comprises the measurements in Rota (Figure5) from June 1989 to December 1989, while the automatic instruments were being installed in the Navy Observatory (Barriendos *et al.*, 2002). This inhomogeneous period continues (although this period contains a short homogeneous period without any explanations due to the few metadata available) until December 1994, when a feasible calibration is achieved in the instruments of the meteorological station.

MONTHS	San Fernando pressure	G+L pressure	G+L pressure minus San Fernando pressure	F <sub>c</sub>	Pressure ((G+L)-SF) - F <sub>c</sub>	Smoothed corrective value
Jan-88	1018.5	1020.9	2.4	3.5	1.1	
Feb-88	1016.7	1020.3	3.6	3.2	-0.4	
Mar-88	1018.4	1021.8	3.4	2.9	-0.4	
Apr-88	1012.8	1015.2	2.4	3.1	0.7	
May-88	1011.8	1014.7	2.9	2.9	0.0	
Jun-88	1011.5	1014.1	2.5	2.9	0.4	
Jul-88	1013.3	1017.1	3.8	3.3	-0.5	
Aug-88	1012.2	1015.4	3.2	3.7	0.5	
Sep-88	1014.0	1018.3	4.3	3.4	-0.9	
Oct-88	1012.6	1015.8	3.1	3.3	0.2	
Nov-88	1012.7	1017.0	4.3	3.4	-0.9	
Dec-88	1022.2	1026.4	4.1	3.4	-0.7	
Jan-89	1024.3	1028.1	3.8	3.5	-0.4	
Feb-89	1020.6	1024.3	3.7	3.2	-0.5	
Mar-89	1014.8	1018.9	4.1	2.9	-1.2	
Apr-89	1011.7	1014.9	3.2	3.1	-0.2	
May-89	1012.6	1016.3	3.6	2.9	-0.7	
Jun-89	1016.6	1016.7	0.1	2.9	<b>2.8</b>	3.2
Jul-89	1016.9	1016.6	-0.3	3.3	<b>3.6</b>	3.4
Aug-89	1015.5	1015.2	-0.3	3.7	<b>3.9</b>	3.7
Sep-89	1015.7	1015.7	-0.1	3.4	<b>3.5</b>	3.5
Oct-89	1018.3	1018.6	0.3	3.3	<b>3.0</b>	3.5
Nov-89	1013.8	1013.2	-0.6	3.4	<b>4.0</b>	4.0
Dec-89	1015.0	1013.5	-1.5	3.4	<b>5.0</b>	4.2
Jan-90	1025.9	1025.8	-0.1	3.5	<b>3.6</b>	3.9
Feb-90	1025.2	1025.3	0.1	3.2	<b>3.1</b>	3.0
Mar-90	1022.8	1023.6	0.7	2.9	<b>2.2</b>	2.8
Apr-90	1016.3	1016.1	-0.2	3.1	<b>3.2</b>	2.7
May-90	1016.3	1016.6	0.2	2.9	<b>2.7</b>	2.8
Jun-90	1016.7	1017.1	0.3	2.9	<b>2.6</b>	2.3
Jul-90	1015.0	1016.9	1.8	3.3	<b>1.5</b>	2.0
Aug-90	1013.7	1017.8	4.1	3.7	-0.4	
Sep-90	1012.9	1016.7	3.8	3.4	-0.4	
Oct-90	1012.6	1015.9	3.3	3.3	0.1	
Nov-90	1014.3	1018.6	4.3	3.4	-0.9	
Dec-90	1014.2	1020.2	5.9	3.4	-2.5	
Jan-91	1020.9	1025.3	4.4	3.5	-0.9	
Feb-91	1017.7	1018.7	1.0	3.2	<b>2.2</b>	2.1
Mar-91	1012.1	1013.1	1.0	2.9	<b>1.9</b>	2.4
Apr-91	1017.9	1017.9	0.0	3.1	<b>3.1</b>	2.3
May-91	1016.9	1017.8	0.9	2.9	<b>2.0</b>	2.3
Jun-91	1016.6	1017.6	1.0	2.9	<b>1.9</b>	2.6
Jul-91	1016.8	1016.3	-0.5	3.3	<b>3.8</b>	3.1
Aug-91	1016.2	1016.3	0.1	3.7	<b>3.6</b>	3.6
Sep-91	1017.0	1017.0	0.0	3.4	<b>3.4</b>	3.6
Oct-91	1017.1	1016.8	-0.3	3.3	<b>3.7</b>	3.6
Nov-91	1021.1	1021.0	-0.2	3.4	<b>3.6</b>	3.5
Dec-91	1024.7	1025.0	0.2	3.4	<b>3.2</b>	3.1
Jan-92	1023.6	1024.6	0.9	3.5	<b>2.6</b>	2.5
Feb-92	1023.4	1024.8	1.4	3.2	<b>1.8</b>	2.0
Mar-92	1020.2	1021.5	1.2	2.9	<b>1.7</b>	1.9
Apr-92	1016.5	1017.3	0.8	3.1	<b>2.3</b>	2.1
May-92	1016.0	1016.6	0.5	2.9	<b>2.4</b>	2.6
Jun-92	1016.3	1016.0	-0.3	2.9	<b>3.2</b>	2.5
Jul-92	1015.7	1016.9	1.2	3.3	<b>2.1</b>	2.8
Aug-92	1017.0	1017.5	0.5	3.7	<b>3.2</b>	2.5
Sep-92	1017.7	1018.8	1.1	3.4	<b>2.4</b>	2.5
Oct-92	1014.4	1015.8	1.3	3.3	<b>2.0</b>	2.0
Nov-92	1023.6	1025.4	1.8	3.4	<b>1.6</b>	1.7
Dec-92	1017.9	1019.8	1.9	3.4	<b>1.5</b>	1.7
Jan-93	1026.9	1028.3	1.4	3.5	<b>2.1</b>	2.1
Feb-93	1020.7	1021.1	0.4	3.2	<b>2.8</b>	2.3
Mar-93	1017.3	1018.1	0.8	2.9	<b>2.1</b>	2.4
Apr-93	1015.5	1016.3	0.7	3.1	<b>2.3</b>	2.3
May-93	1013.9	1014.4	0.5	2.9	<b>2.4</b>	2.3
Jun-93	1016.9	1017.6	0.7	2.9	<b>2.2</b>	2.1
Jul-93	1015.7	1017.4	1.7	3.3	<b>1.6</b>	2.3
Aug-93	1015.5	1016.2	0.7	3.7	<b>3.0</b>	2.4
Sep-93	1016.1	1016.9	0.8	3.4	<b>2.6</b>	2.8
Oct-93	1014.5	1015.1	0.5	3.3	<b>2.8</b>	2.5
Nov-93	1016.8	1018.0	1.2	3.4	<b>2.2</b>	2.3
Dec-93	1024.0	1025.4	1.4	3.4	<b>2.0</b>	1.8
Jan-94	1021.7	1024.1	2.4	3.5	<b>1.1</b>	2.2
Feb-94	1019.2	1019.0	-0.2	3.2	<b>3.4</b>	1.8
Mar-94	1020.1	1022.2	2.0	2.9	<b>0.9</b>	1.9
Apr-94	1017.0	1018.6	1.6	3.1	<b>1.5</b>	2.1
May-94	1015.4	1014.6	-0.9	2.9	<b>3.8</b>	2.5
Jun-94	1017.5	1018.2	0.7	2.9	<b>2.2</b>	3.0
Jul-94	1015.7	1016.1	0.4	3.3	<b>2.9</b>	2.9
Aug-94	1015.4	1015.6	0.2	3.7	<b>3.5</b>	3.1
Sep-94	1016.0	1016.5	0.4	3.4	<b>3.0</b>	3.1
Oct-94	1015.4	1015.9	0.5	3.3	<b>2.9</b>	3.0
Nov-94	1020.9	1021.1	0.1	3.4	<b>3.3</b>	3.2
Dec-94	1026.4	1026.3	-0.2	3.4	<b>3.6</b>	3.4
Jan-95	1024.0	1027.2	3.2	3.5	0.3	
Feb-95	1021.0	1024.1	3.1	3.2	0.1	
Mar-95	1015.0	1018.9	3.9	2.9	-0.9	
Apr-95	1012.7	1016.2	3.5	3.1	-0.4	
May-95	1013.3	1016.5	3.2	2.9	-0.2	
Jun-95	1012.2	1014.5	2.3	2.9	0.6	
Jul-95	1012.1	1015.2	3.1	3.3	0.2	
Aug-95	1011.8	1014.6	2.8	3.7	0.9	
Sep-95	1013.9	1017.1	3.2	3.4	0.2	
Oct-95	1015.9	1019.0	3.1	3.3	0.3	
Nov-95	1014.0	1017.4	3.4	3.4	0.0	
Dec-95	1012.1	1015.0	2.9	3.4	0.5	

**Table 3.** Divergence calculation between San Fernando and G+L pressures and corrective value for each month of the 1988-1995 period. (The anomalous months are written in bold).



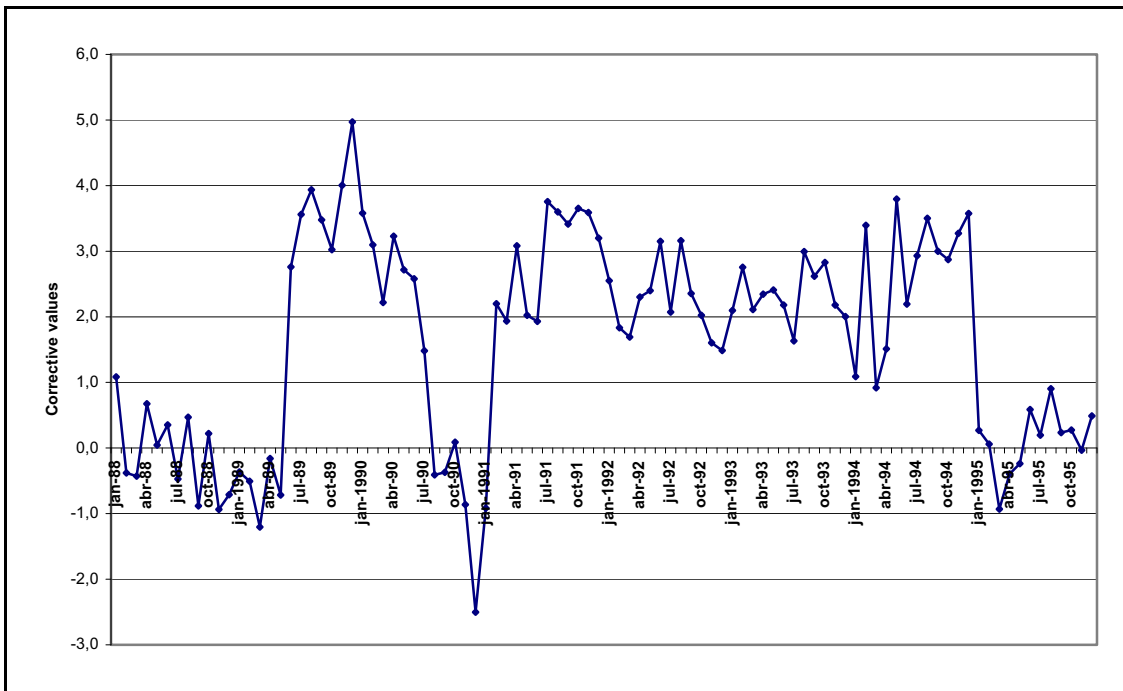


**Figure 9.** Corrective values representation for each month individually from January 1988 to December 1995.

1.3.2.3. The homogenised San Fernando pressure series graphic

The San Fernando mean annual pressure series is shown for the whole study period (Figure 10). The first period shows low values, but they increase at the beginning of the 20th century and decrease during the ‘1960s and ‘1970s, and recover at the end of the century. During the study period are lacking 95 days (0.14% out of the 65.744 total days). Comparing San Fernando and Padua series (Figure 4), the standard deviation is higher in Padua than in San Fernando because winter anticyclones alternates with orographical lows over the Gulf of Genoa. San Fernando is predominantly under the Azores anticyclone, except for those winter episodes when a circumpolar low detaches towards the Mediterranean latitudes.

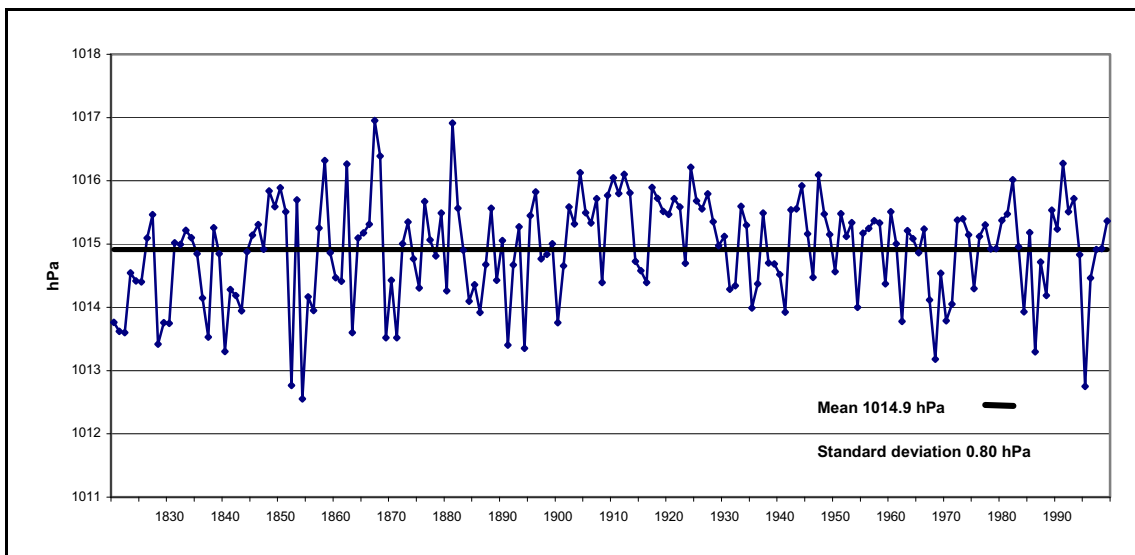


**Figure 10.** Mean annual pressure in San Fernando (1821-2000).

## 1.4. THE WeMO TRANSECT

A line from San Fernando to Padua is drawn. This segment is almost parallel to the Catalan Countries shoreline. Moreover, the study area is exactly in the middle of the transect (Figure 11). For this thesis, several analyses include the NAO to compare with the WeMO, since it was the main reason to define this new teleconnection pattern.

For the north extreme of the NAO dipole, Reykjavik is used on the south-western Iceland coast, whilst for the southern extreme, one of several can be used: Ponta Delgada, Lisboa or Gibraltar. In the monthly and annual analyses, the Gibraltar series is considered (Jones *et al.*, 1997, CRU). This location is quite near to the Gulf of Cadiz, therefore, it is useful to rotate the NAO transect eastward towards the western Mediterranean basin. In daily analyses, depending on the daily data available, the San Fernando series is used instead of Gibraltar, and Sttykishólmur instead of Reykjavik (western Iceland coast). The WeMO transect is approximately the middle of the NAO transect on the map (UTM projection) of the Figure 11. The WeMO must be considered as a regional teleconnection pattern.

The extremes of a pattern dipole should be anti-correlated, but it does not happen with the WeMO (Table 4) because San Fernando and Padua are in the same half of the Rossby wavelength, which fits exactly with the whole Mediterranean basin length (Maheras *et al.*, 1999a and 1999b). Consequently, both series are positively correlated, corroborating the regional feature of the pattern.



**Figure 11.** Segments linking the representative meteorological stations of the NAO and WeMO dipoles. (Universal Transversa Mercator –UTM– Projection, Datum European 1950, 31N).

Jan	Feb	Mar	Abr	Mai	Jun	Jul	Aug	Sep	Oct	Nov	Dec	<b>Annual</b>
0.57	0.58	0.52	0.27	0.40	0.41	0.31	0.39	0.35	0.44	0.37	0.43	<b>0.41</b>

**Table 4.** Correlation between the San Fernando and Padua pressure series (1821-2000).

## 1.5. WeMOi VALUES CALCULATION

### 1.5.1. MONTHLY, SEASONAL AND ANNUAL RESOLUTION

The index calculation is achieved by standardising each dipole series separately. A mean of all daily pressure values is worked out in order obtain a monthly pressure value. Afterwards, the mean pressure for the 1961-1990 reference period of one specific month must be subtracted from this value. Finally, the result must be divided by the standard deviation of the specific month for the same reference period (1961-1990). To obtain the normalised WeMOi value (Z), the Padua value must be subtracted from the standardized San Fernando value, implying the positive values to be related to the positive WeMO phase (Figure 1).

E.g. January 1981 WeMOi,

$$Z_{\text{WeMOi Jan 1981}} = \left\{ \left( P_{\text{Jan 1981 SF}} - X_{\text{SF 1961-1990}} \right) / \delta_{\text{SF 1961-1990}} \right\} - \left\{ \left( P_{\text{Jan 1981 PD}} - X_{\text{PD 1961-1990}} \right) / \delta_{\text{PD 1961-1990}} \right\},$$

where P, pressure, SF, San Fernando, PD, Padua, X, mean and  $\delta$ , standard deviation.

To calculate the seasonally values, the mean of the monthly standardised values of each season is worked out. The annual value is obtained reckoning the 12 monthly standardised values.

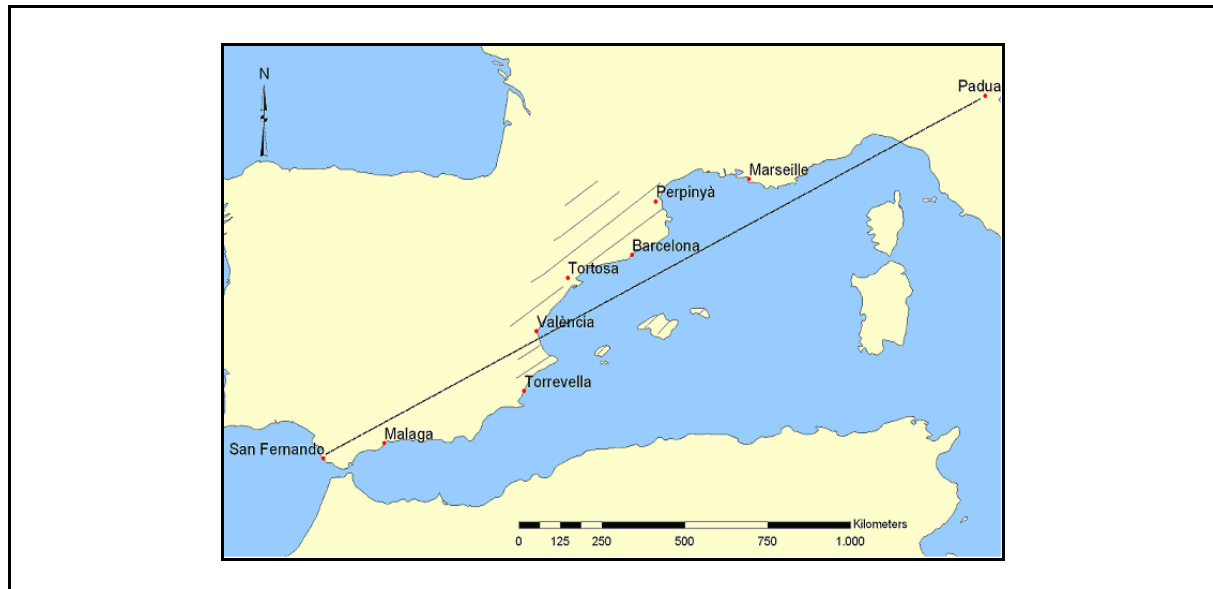
### 1.5.2. DAILY RESOLUTION

#### 1.5.2.1. Calculation process

The daily WeMOi application is a methodological contribution of the current thesis. It is a new tool, since it converts the low frequency feature of the teleconnection patterns into a high frequency. It is coherent to be applied at our latitudes where the pressure behaviour is usually regular (Gil Olcina and Olcina Cantos, 1997). There are few antecedents in using patterns at a daily resolution (Baldwin and Dunkerton, 2001; Lopez-Bustins and Azorin-Molina, 2005; Martin-Vide and Lopez-Bustins, 2006; Peña *et al.*, 2006a). Even Camuffo *et al.* (2006) have done some applications with daily WeMOi as they compare it with the day-to-day Padua pressure variability.

To define the daily WeMOi calculation process, 7 reference meteorological stations are employed along the north-western Mediterranean shoreline: Marseille, Perpinyà, Barcelona, Tortosa, València, Torrevella and Malaga. The daily precipitation for the 1951-2000 period is

used. 5 out of the 7 series are in the Catalan Countries; the other two are northward (Marseille) and southward (Malaga). These series are used for the daily precipitation analyses throughout the thesis, and are considered as the main meteorological stations due to their reliability. 6 out of the 7 series have been assessed within the European Climate Assessment & Dataset (ECA&D) project (Figure 12).



**Marseille** (France): North of the Catalan Countries. 43:18:18N-05:23:48E. Source: ECA&D. Unique series from the *Palais-Lonchamp* Observatory. 75 m a.s.l. Station number and code: 97/13055001. 99.63% data available.

**Perpinyà**: Northern Catalan Countries. 42:44:18N-02:52:24E. Source: ECA&D. Unique series from Llavanera aerodrome. 42 m a.s.l. Station number and code: 117/66136001. 100% data available.

**Barcelona**: North-eastern Catalan Countries. 41:25:05N-02:07:27E. Source: Spanish Meteorological Office and Annual Bulletins of the observatory. Unique series from the Fabra Observatory (Collserola Hill). 420.11 m a.s.l. Code station: 200E. 100% data available.

**Tortosa**: Mid-Catalan Countries. 40:49:14N-00:29:29E. Source: Spanish Meteorological Office and ECA&D. Unique series from Ebre Observatory in Roquetes. 48 m a.s.l. Station number and code: 729/9981A. 100% data available.

**València**: Mid-southern Catalan Countries. 39:28:48N-00:22:52W. Source: Spanish Meteorological Office and ECA&D. Unique series from ‘Els Vivers’. 11 m a.s.l. Station number and code: 732/8416. 100% data available.

**Torrevella**: Southern Catalan Countries. 37:58:38N-00:42:39W. Source: ECA&D. Unique series from the Torrevella lagoon. 1 m a.s.l. Station number and code: 726/7038. 100% data available.

**Málaga** (Spain): South of the Catalan Countries. 36:40:00N-04:29:17W. Source: ECA&D. Unique series from the Malaga airport. 7 m a.s.l. Station number and code: 713/6155. 100% data available.

**Figure 12.** Localization map of the daily precipitation reference meteorological stations in the synoptic framework of the western Mediterranean basin.

The selected method consists of standardising each series of the dipole previously. The mean and the standard deviation of the 1961-1990 period of the all days of the year (from 1st January 1961 to 31st December 1990) must be used.

E.g. 1<sup>st</sup> January 1981 WeMOi,

$$Z_{\text{WeMOi 1st Jan 1981}} = \left\{ \left( P_{1^{\text{st}} \text{ Jan SF}} - X_{\text{SF 1961-1990}} \right) / \delta_{\text{SF 1961-1990}} \right\} - \left\{ \left( P_{1^{\text{st}} \text{ Jan PD}} - X_{\text{PD 1961-1990}} \right) / \delta_{\text{PD 1961-1990}} \right\},$$

where P, pressure, SF, San Fernando, PD, Padua, X, mean, and  $\delta$ , standard deviation.

This calculation method allows us to detect those easterly flows (negative WeMO phase), even if they are very weak. Otherwise, those moderate episodes would not be detected in autumn, since the WeMOi means are very negative during this season. In the same way, those weak episodes would be overestimated in winter due to the high WeMOi mean in this season (Figure 21 in the 2nd chapter). Table 5 shows that the method selected, among the 9 proposed, is the **An**, which obtains the best correlation in all the meteorological stations. Further information about the An and the other methods put forward is in the original Catalan version of the thesis.

1951-2000	Marseille	Perpignan	Barcelona	Tortosa	València	Torrevela	Malaga
<b>Dr</b>	-0.075	-0.160	-0.137	-0.194	-0.185	-0.125	-0.237
<b>Ms</b>	-0.079	-0.167	-0.146	-0.203	-0.192	-0.129	-0.251
<b>St</b>	-0.078	-0.168	-0.149	-0.202	-0.193	-0.125	-0.258
<b>An</b>	<b>-0.086</b>	<b>-0.180</b>	<b>-0.172</b>	<b>-0.217</b>	<b>-0.208</b>	<b>-0.134</b>	<b>-0.273</b>
<b>RPDr</b>	-0.036	-0.134	-0.105	-0.165	-0.164	-0.109	-0.193
<b>RPMs</b>	-0.039	-0.141	-0.112	-0.173	-0.170	-0.114	-0.200
<b>RPSt</b>	-0.042	-0.144	-0.118	-0.175	-0.174	-0.113	-0.206
<b>RPAAn</b>	-0.054	-0.159	-0.144	-0.194	-0.194	-0.127	-0.223
<b>RS</b>	-0.054	-0.159	-0.144	-0.194	-0.194	-0.127	-0.223

**Table 5.** Correlation coefficients (r-Pearson) between the different daily WeMOi values and the daily precipitation of the 7 reference observatories during the 1951-2000 period.

#### 1.5.2.2. Daily WeMOi frequencies distribution (1951-2000)

The 1951-2000 period was selected to analyse the daily WeMOi frequencies distribution. This period comprises 18.182 days which have a WeMOi value (99.6%), +5.99 being the superior threshold and -5.90 the inferior threshold. The intervals class is 0.25, whilst the modal class is (-0.25, 0). Although the distribution looks quite symmetrical, it has got no

Gaussian distribution according to the Kolmogorov-Smirnov test due to the high number of WeMOi values considered (18.182 days) ( $D_{\max} = 0.0465572$ ) (Figure 13). Nevertheless, Skew (+0.26) and Kurtosis (+1.20) coefficients do not show any significant distance from normality as they are between -2 and 2. The first one shows daily WeMOi values to be positively skewed. It is displayed in the histogram as the extreme positive values are more frequent than the negative ones, but the major concentration cases is in slight negative intervals, (-0.25, 0) and (-0.5, -0.25). The positive Kurtosis coefficient is reflected with a leptokurtic histogram.

The numbers of days with a positive WeMOi value (8,554 days, 47.0%) and a negative value (9,628 days, 53.0%) are both around 50% of the total number of days. This percentual equilibrium between the positive and negative values even improves in longer periods. The 1870-2000 period comprises 47,263 days (98.8% of 47,847 total days), 23,443 days of them (49.6%) have a positive WeMOi value, and 3,820 days (50.4%) a negative one. 64,295 days (97.8% of 65,744 total days) have a WeMOi value in the period 1820-2000, in 31,731 days (49.4%) with a positive value and in 32,564 days (50.6%) with a negative value. The predominance of the negative values of daily WeMOi is a relevant feature in all periods.

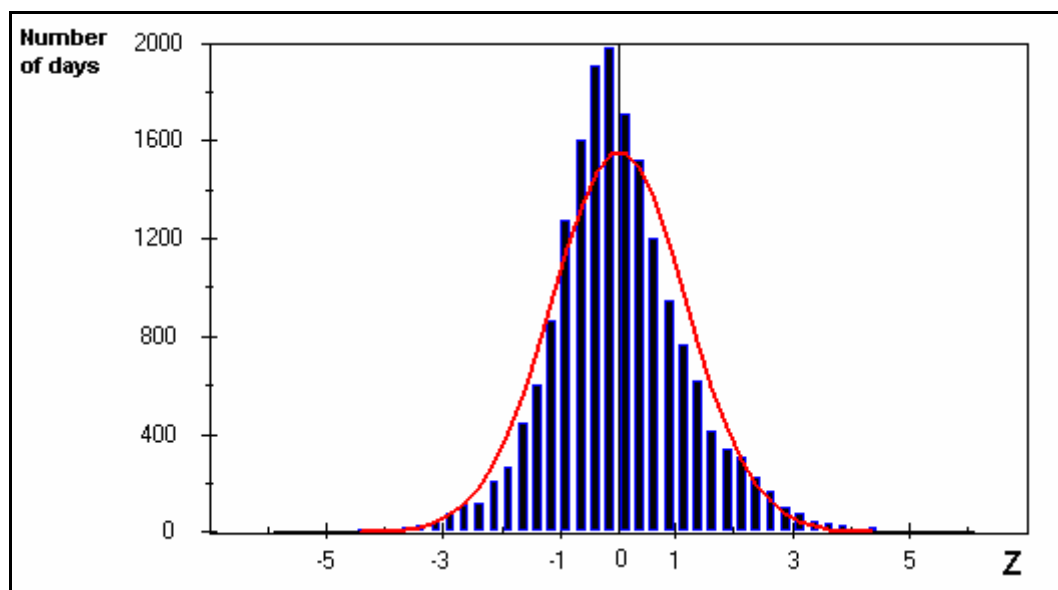


**Figure 13.** Daily WeMOi frequencies histogram (1951-2000) and Gaussian distribution adjustment. (The distance between class intervals is 0.25)<sup>1</sup>.

<sup>1</sup> The interval classes of the frequency distributions of daily WeMOi values can be open and close simultaneously. These values always have several decimals as they are the result of a subtraction of normalised values. The daily WeMOi values will never be integers.

## 1.6. WeMOi TEMPORAL EVOLUTION (1821-2000)

The same as other patterns of the northern hemisphere, the WeMO is most dynamical during the cold half of the year. The winter WeMOi analysis, from December to March, shows phases of opposed sign with a 3rd degree polynomial regression (Figure 14). During all the 19th century, the WeMO shows a phase with mostly negative values, even beyond the Urrutia Brothers's period. On the other hand, since the beginning of the 20th century to the end of the '60s the phase is positive. Along the three last decades of the 20th century, there is an alternation of years with positive and negative WeMOi values, but with an overall negative trend. Despite the inhomogeneties remaining in the Urrutia Brothers's period, some historical studies on climatology point out frequent severe weather in eastern Iberia during the mid-19th century due to the last oscillations of the Little Ice Age (Oliva *et al.*, 2006), which might explain why there were lots of consecutive years with a negative WeMOi value in that period.

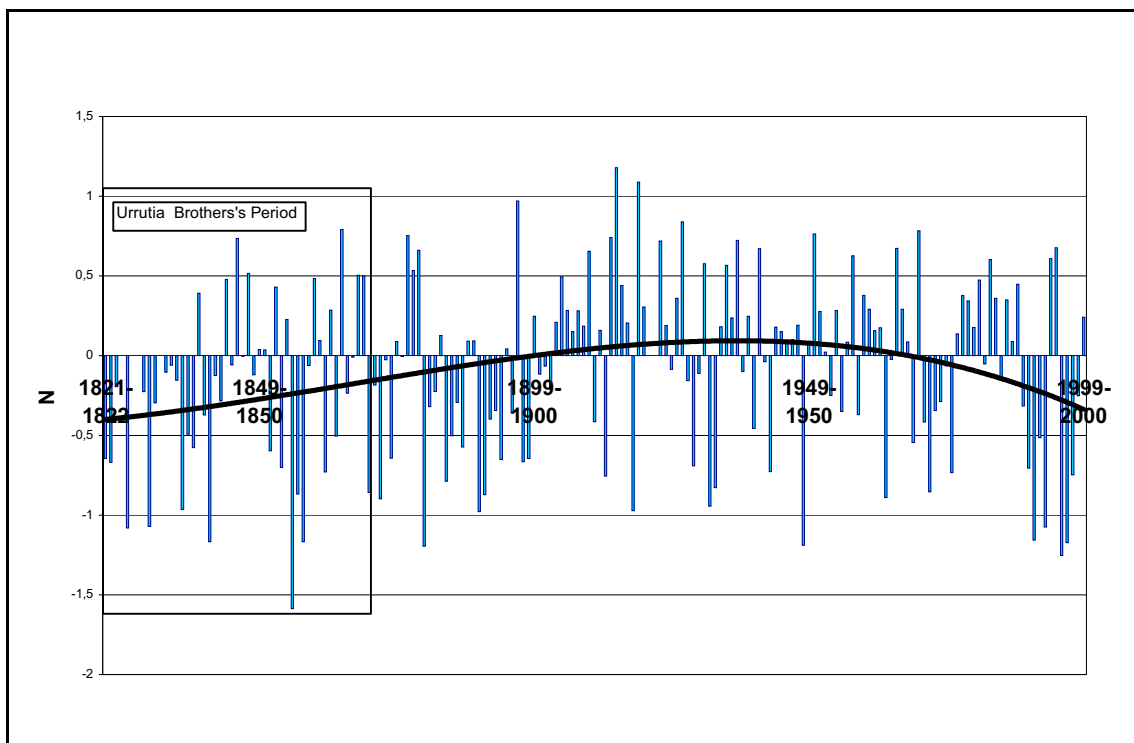


**Figure 14.** Winter WeMOi evolution (December, January, February and March) (1821/1822-1999/2000).

## 1.7. WeMOi CORRELATION AND VALIDATION WITH OTHER INDICES

The WeMO shows a clear independence from the external dynamics to the Mediterranean basin. Although there is a positive correlation between the NAOi and the WeMOi in winter, it is not significant at 0.05 (Table 6). The same happens with the East Atlantic oscillation (EA). The WeMOi is negative and significantly correlated with the AOi ( $r = -0.39$ ,  $p$ -value = 0.0055), and with the Eurasian-1 index (EU-1) too, but weakly ( $r = -0.30$ ,  $p$ -valor = 0.0379). Consequently, a certain influence of the polar vortex is deduced, but in an opposed way. El Niño – Southern Oscillation (ENSO) shows a slight negative relationship, not significant, with the WeMOi, and the QBO does not show any. The WeMOi does not correlate with MOi significantly either, but a significant positive correlation has been obtained in some winter months (not shown).

These results validate the research and formulation of a novel teleconnection pattern for the western Mediterranean basin, since the WeMOi is connected with nearby patterns, but weakly. I highlighted the WeMO role on distinguishing the NAO behaviour from that one of the AO, as it is quite differently related to them. It must be kept in mind that the NAOi and the AOi are highly correlated as the AO is the poleward mode of the NAO.

		MO	NAO	AO	EU-1	EU-2	EA	ENSO	QBO
WeMOi	Pearson's correlation coefficient	+0.0249	+0.1220	-0.3866	-0.2945	-0.2424	+0.1332	-0.0971	-0.0583
	p-value	0.8666	0.3988	<b>0.0055</b>	<b>0.0379</b>	0.0898	0.3566	0.5023	0.6972

**Table 6.** Pearson's correlation coefficients between the WeMOi and the indices of other patterns in winter (from December to March) for the 1950/51-1999/2000 period ( $p$ -values are displayed; those ones significant at 0.05 are in bold). Data source: MO (Dünkeloh and Jacobeit, 2003) (MO data end in 1998), NAO (Jones *et al.*, 1997), AO (Thompson and Wallace, 2000), EU-1 (NOAA), EU-2 (NOAA), EA (NOAA), ENSO (Trenberth and Stepaniak, 2001) and QBO (Marquardt and Naujokat, 1997) (QBO data begin in 1953).

To corroborate the opposed significant relationship between the AOi and the WeMOi in winter, the study period has been double enlarged for the whole 20th century. The results show a maintenance in the correlation coefficient, even reinforcing the significance ( $r = -0.2956$ ,  $p$ -valor = 0.0031). The dots cloud shows an inversely proportional relationship as the linear regression indicates,  $WeMOi = -0.165AOi + 0.022$  (Figure 15).



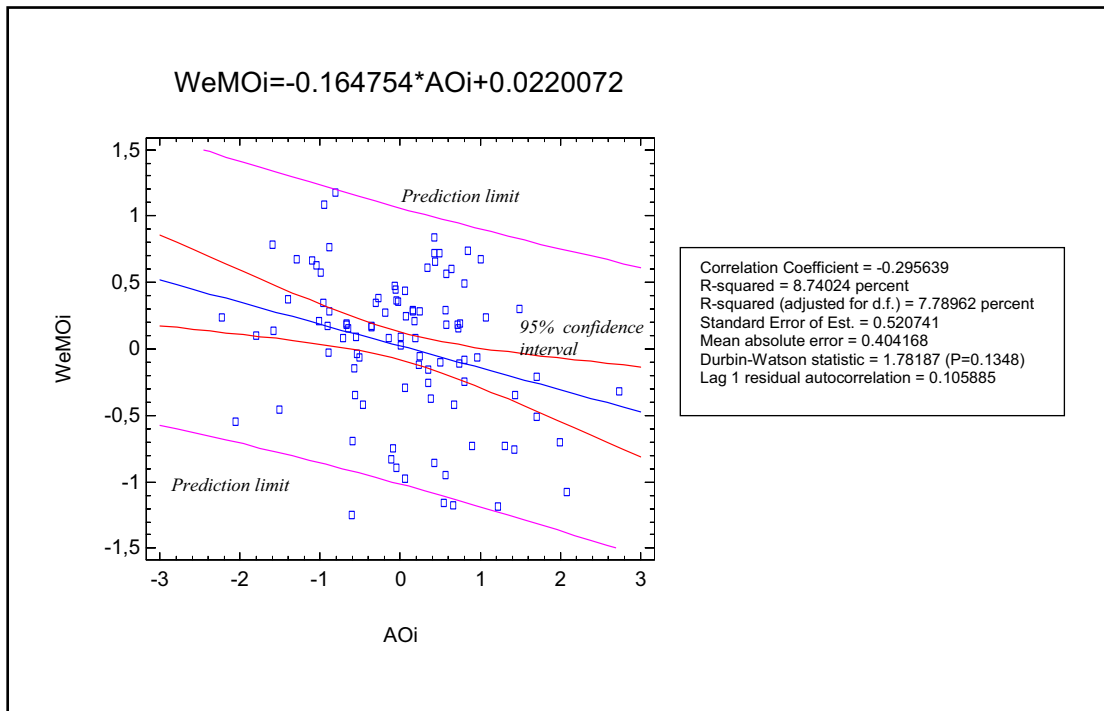


**Figure 15.** Linear regression between the WeMOi and the AOi in winter (from December to March) for the 1900/01-1999/2000 period.